In Situ Observations of Water Production and Distribution in an Operating H₂/O₂ PEM Fuel Cell Assembly Using ¹H NMR Microscopy

Kirk W. Feindel, Logan P.-A. LaRocque, Dieter Starke, Steven H. Bergens,* and Roderick E. Wasylishen*

Department of Chemistry, University of Alberta, Edmonton, Alberta, Canada T6G 2G2

Received June 30, 2004; E-mail: steve.bergens@ualberta.ca; roderick.wasylishen@ualberta.ca

Proton NMR microscopy[1] was applied to investigate in situ the production and distribution of water in an operating H_2/O_2 polymer electrolyte membrane fuel cell (PEMFC). The distribution of water in operating PEMFCs, or a series thereof (i.e., stack), must be carefully managed to optimize the performance, durability, and functionality (e.g., freeze-start) of the system. For example, the ionic conductivity of polymer electrolyte membranes (PEMs) decreases as membrane hydration is reduced.[2,3] Flooding the cathode catalyst inhibits mass transport and can lead to failure of materials.[4,5] Further, buildup of water in the gas channels (i.e., flow fields) of a stack of fuel cells will create a nonuniform distribution of pressure drops across the individual cells.[4]

Water is present in the flow fields, catalysts, membrane, and gas diffusion layers of an operating PEMFC. The reported experimental methods used to study water in the membrane between the catalysts of operating PEMFCs include water transfer measurements,[2,4,5] conductivity measurements,[3] neutron imaging,[6] and ¹H NMR imaging.[7] In recent reports, Panchenko et al.[8] studied degradation of the PEM in fuel cells operating in an EPR spectrometer. To our knowledge, there are only two reports of direct observations of water in the diffusion layers and flow fields of operating PEMFCs. Satija et al.[9] used neutron imaging in their study involving a stack of H_2/O_2 PEMFCs, while Tüber et al.[10] constructed a transparent H_2/O_2 PEMFC to allow direct visual observation of water distribution.

The nondestructive nature of NMR spectroscopy enables one to obtain unique in situ information from a multitude of systems.[1,11] Babu et al.[12] have studied the electronic properties of fuel cell catalysts via electrochemical NMR. Water dynamics,[13,14] electroosmotic drag,[15] and the sorption and diffusion of water or methanol[16,17] in PEMs have been studied by ¹H NMR spectroscopy. Proton NMR microscopy has been used to illustrate the electrically induced diffusion of water in Nafion membranes.[18] Also, Teranishi et al.[7] initiated the use of ¹H NMR microscopy for investigating the distribution of water in Aciplex membranes between Pt on carbon electrodes operating on H_2/O_2. We now report the use of ¹H NMR microscopy to examine in a single experiment the distribution of water throughout an operating H_2/O_2 PEMFC. The areas investigated include the flow fields, current collectors, membrane electrode assembly (MEA), and the membrane surrounding the catalysts.

The MEA used for this study was constructed with a standard Nafion 117 membrane and a hot-press decal transfer method.[19,20] Pt black (Johnson Matthey HiSPEC 1000, specific surface area 27 $m^2\ g^{-1}$) and Pt−Ru black (Johnson Matthey HiSPEC 6000, specific surface area 70 $m^2\ g^{-1}$) were used as the cathode and anode catalyst, respectively. The fuel cell assembly was designed to fit in a 30 mm diameter birdcage coil, with the plane of the PEM parallel with the applied magnetic field. The cell hardware consisted of Delrin cylinder halves with machined flow fields, gold contacts, and Toray carbon paper current collectors. The performance of the fuel cell, voltage versus current, operating on H₂(humidified)/O₂
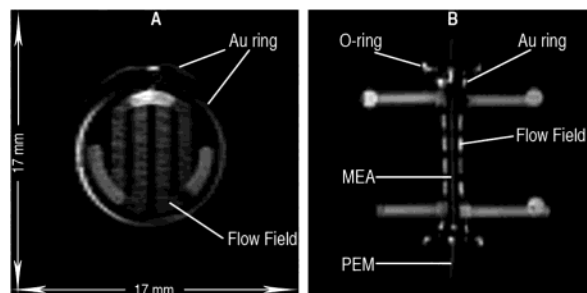
Figure 1. Images of the fuel cell flooded with water obtained with a SE sequence, pixel size = $133 \times 234\ \mu m$. Labels indicate location of water with respect to hardware. (A) A 0.8 mm slice containing the flow field only; outer rings are from water pooling around the Au wire. (B) A 1.0 mm axial slice illustrating the water-saturated MEA and PEM (obtained after immersing a conditioned, operated fuel cell in water).

at ambient temperature was stable after conditioning.[19] Proton NMR images were acquired[21] at 300.4 MHz with a Bruker Avance console and Micro 2.5 imaging accessory using a 1 T m^{-1} maximum gradient strength. Standard gradient echo fast imaging[22] (GEFI) or multislice[23] spin−echo (SE) imaging sequences were used. For water in Nafion at 293 K, MacMillan et al.[13] determined ¹H T_1 values ranging from 0.2 to 1 s, increasing with the level of hydration. During fuel cell operation, the amount of water in the membrane fluctuates. For imaging sequences involving spin−echoes with $\pi/2$ excitation pulses, we determined that repeat times of 2 s were sufficient to prevent saturation of the ¹H NMR signal. The performance of the fuel cell measured outside of the applied magnetic field and during image acquisition was identical. We believe that the minuscule amount of heat generated by the cell was dissipated through the flowing gases and the fuel cell/probe assembly.

Filling the anode and cathode flow fields with water allows rapid image acquisition to determine the alignment of the fuel cell within the magnet and to check the system for leaks and blockages. Figure 1 contains images of the water-filled flow field and of an axial cross-section showing the water-saturated membrane in the region pressed between the catalysts (MEA) and in the regions surrounding the catalysts.

Images of the operating fuel cell were obtained after flushing water from the anode and cathode flow fields with humidified H₂ and dry O₂ until the amount of water imaged in the membrane was constant. Figure 2 shows images of the membrane region inside and around the MEA. The image in Figure 2A was recorded with the fuel cell at a potential of ∼1 V before current was passed through the cell; therefore, this image represents the amount of water in the membrane as established by the humidified H₂ and dry O₂.

Figure 2B is an image of the same membrane region acquired after the fuel cell was operated for 6 h at ∼52 mA cm⁻² and ∼0.73 V. Comparison of the images in Figures 2A and 2B shows that the amount of water in the membrane surrounding the MEA and outside
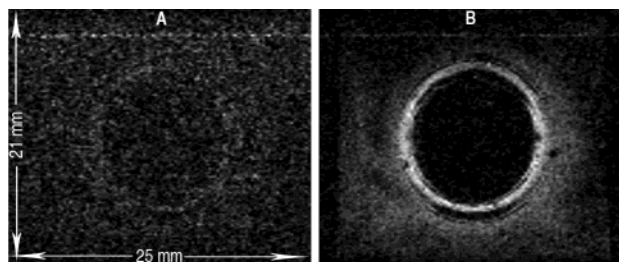
Figure 2. Membrane inside and around the MEA: (A) before current was passed through the cell and (B) after operating the fuel cell at ~52 mA cm^{-2} and ~0.73 V for 6 h. Comparison of images A and B demonstrates the diffusion of water through the Nafion membrane away from the MEA. GEFI sequence, 0.7 mm slice, pixel size = 164 × 234 μm, acquisition time = 13.8 min.
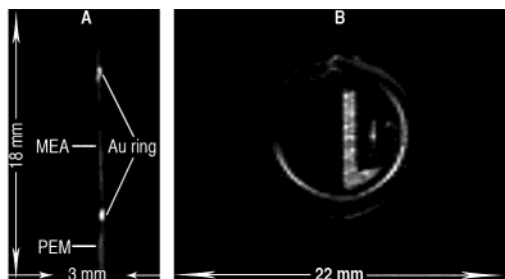
Figure 3. Images of the fuel cell operating at ~52 mA cm^{-2} and ~0.73 V acquired with a SE sequence. (A) A 1.0 mm axial slice after ~30 h, pixel size = 15 × 234 μm, acquisition time = 13.65 h. (B) View of partially blocked cathode flow field after ~72 h; outside rings indicate pooling of water around the Au ring; 0.7 mm slice, pixel size = 172 × 234 μm, acquisition time = 17 min.

the O-ring seals increases during operation of the fuel cell. Thus, a portion of the water formed at the cathode and brought into the membrane by electroosmotic drag from the anode diffuses radially down the concentration gradient through the membrane away from the MEA. This observation suggests that radial gradient diffusion will reduce flooding at cathode sites near the edges of MEAs and decrease the amount of water in the membrane pressed between the catalysts.

To observe water in the cathode flow field, the fuel cell was imaged intermittently while operating under a constant load (~52 mA cm^{-2} and ~0.73 V) for 96 h. The image in Figure 3A shows the presence of water in the MEA, the surrounding membrane, and water pooled around the Au wire. This image clearly shows that the distribution of water in the membrane was not uniform. Previous reports demonstrate that the equilibrium concentration for water in Nafion is higher when the membrane is in contact with liquid water than when in contact with saturated water vapor.[2] As shown by the image in Figure 3A, less water is contained in the MEA than in the region of the membrane in direct contact with water pooled around the gold ring contact. Buildup of water in the cathode flow field was observed to create transient obstructions during operation of the cell. Figure 3B shows such an obstruction before it was flushed by the O$_2$ stream. Water obstructions were also observed (not shown) in the anode flow field when the humidity of the H$_2$ stream was too high.

The results presented in this study demonstrate that unique information regarding the distribution of water throughout an operating fuel cell assembly can be obtained using ^{1}H NMR microscopy. For the first time, radial gradient diffusion of water from the MEA into the surrounding Nafion membrane was observed. The results show that ^{1}H NMR microscopy is a powerful technique that will aid the design of fuel cell flow fields and components to optimize water management. Further research is underway in our laboratories to better quantify the NMR microscopy data obtained from operational fuel cells.

References

(1) (a) Watanabe, T. *Nucl. Magn. Reson.* **2003**, *32*, 433−472. (b) Blümich, B. *NMR Imaging of Materials*; Oxford University Press: New York, 2000. (c) Callaghan, P. T. *Principles of Nuclear Magnetic Resonance Microscopy*; Oxford University Press: New York, 1991.
(2) Zawodzinski, T. A.; Derouin, C.; Radzinski, S.; Sherman, R. J.; Smith, V. T.; Springer, T. E.; Gottesfeld, S. *J. Electrochem. Soc.* **1993**, *140*, 1041−1047.
(3) Cappadonia, M.; Erning, J. W.; Niaki, S. M. S.; Stimming, U. *Solid State Ionics* **1995**, *77*, 65−69.
(4) Büchi, F. N.; Srinivasan, S. *J. Electrochem. Soc.* **1997**, *144*, 2767−2772.
(5) (a) Choi, K.-H.; Peck, D.-H.; Kim, C. S.; Shin, D.-R.; Lee, T.-H. *J. Power Sources* **2000**, *86*, 197−201. (b) Janssen, G. J. M.; Overvelde, M. L. J. *J. Power Sources* **2001**, *101*, 117−125. (c) Sena, D. R.; Ticianelli, E. A.; Paganin, V. A.; Gonzalez, E. R. *J. Electroanal. Chem.* **1999**, *477*, 164−170.
(6) Bellows, R. J.; Lin, M. Y.; Arif, M.; Thompson, A. K.; Jacobson, D. *J. Electrochem. Soc.* **1999**, *146*, 1099−1103.
(7) (a) Teranishi, K.; Tsushima, S.; Hirai, S. *Therm. Sci. Eng.* **2003**, *11*, 35−36. (b) Teranishi, K.; Tsushima, S.; Hirai, S. *Therm. Sci. Eng.* **2002**, *10*, 59−60.
(8) (a) Panchenko, A.; Dilger, H.; Kerres, J.; Hein, M.; Ullrich, A.; Kaz, T.; Roduner, E. *Phys. Chem. Chem. Phys.* **2004**, *6*, 2891−2894. (b) Panchenko, A.; Dilger, H.; Möller, E.; Sixt, T.; Roduner, E. *J. Power Sources* **2004**, *127*, 325−330.
(9) Satija, R.; Jacobson, D. L.; Arif, M.; Werner, S. A. *J. Power Sources* **2004**, *129*, 238−245.
(10) Tüber, K.; Pócza, D.; Hebling, C. *J. Power Sources* **2003**, *124*, 403−414.
(11) See for example: (a) Weekley, A. J.; Bruins, P.; Augustine, M. P. *Am. J. Enol. Vitc.* **2002**, *53*, 318−321. (b) Brouwer, E. B.; Moudrakovski, I.; Chung, K. H.; Pleizier, G.; Ripmeester, J. A.; Deslandes, Y. *Energy Fuels* **1999**, *13*, 1109−1110.
(12) Babu, P. K.; Kim, H. S.; Oldfield, E.; Wieckowski, A. *J. Phys. Chem. B* **2003**, *107*, 7595−7600 and references therein.
(13) MacMillan, B.; Sharp, A. R.; Armstrong, R. L. *Polymer* **1999**, *40*, 2471−2480.
(14) MacMillan, B.; Sharp, A. R.; Armstrong, R. L. *Polymer* **1999**, *40*, 2481−2485.
(15) Ise, M.; Kreuer, K. D.; Maier, J. *Solid State Ionics* **1999**, *125*, 213−223.
(16) Jayakody, J. R. P.; Stallworth, P. E.; Mananga, E. S.; Farrington-Zapata, J.; Greenbaum, S. G. *J. Phys. Chem. B* **2004**, *108*, 4260−4262.
(17) Hietala, S.; Maunu, S. L.; Sundholm, F. *J. Polym. Sci., Part B: Polym. Phys.* **2000**, *38*, 3277−3284.
(18) Baker, R. T.; Naji, L.; Lochhead, K.; Chudek, J. A. *Chem. Commun.* **2003**, 962−963.
(19) Cao, D. X.; Bergens, S. H. *Electrochim. Acta* **2003**, *48*, 4021−4031.
(20) Ren, X.; Wilson, M. S.; Gottesfeld, S. *J. Electrochem. Soc.* **1996**, *143*, L12−L15.
(21) For the GEFI and SE pulse sequences, repetition times of 200 ms and 2−3 s and minimum echoes times of 1.9 ms and 3.0−5.2 ms were used, respectively.
(22) Haase, A.; Frahm, J.; Matthaei, D.; Hänicke, W.; Merboldt, K.-D. *J. Magn. Reson.* **1986**, *67*, 258−266.
(23) Frahm, J.; Merboldt, K. D.; Hänicke, W.; Haase, A. *J. Magn. Reson.* **1985**, *64*, 81−93.

JA0461116